

Wavelength-scanning digital interference holography for tomographic three-dimensional imaging by use of the angular spectrum method

Lingfeng Yu and Myung K. Kim

Department of Physics, University of South Florida, Tampa, Florida 33620

Received April 4, 2005

A tomographic imaging system based on wavelength-scanning digital interference holography is developed by applying the angular spectrum method. Compared to the well-known Fresnel diffraction formula, which is subject to a minimum distance requirement in reconstruction, the angular spectrum method can reconstruct the wave field at any distance from the hologram plane. The new system allows three-dimensional tomographic images to be extracted with an improved signal-to-noise ratio, a more flexible scanning range, and an easier specimen size selection. Experiments are performed to demonstrate the effectiveness of the method. © 2005 Optical Society of America

OCIS codes: 110.6960, 090.1760, 110.6880.

Imaging techniques that reveal the tomographic structure of biological or material tissues by use of optical radiation has become a subject of increasing interest. Optical coherence tomography (OCT)¹ is an effective interferometric technique that can produce high-resolution cross-sectional images of biological structures. This method is based on the measurement of the interferometric cross correlation of the light backscattered from the sample with the light retroreflected from the reference mirror. The three-dimensional image is reconstructed by scanning the three dimensions pixel by pixel. Although microscanning with piezoactuators is a well-established art, being able to obtain images frame by frame will have obvious technical advantages. Wide-field two-dimensional OCT has been developed as a method of acquiring a sequence of full-field interferometric images by illumination with a broadband light source, generating the optical section images,^{2,3} which can be in natural color representation.⁴

We have been developing an alternative approach called wavelength-scanning digital interference holography (WSDIH), where holographic images of an object volume are numerically reconstructed with the well-known Fresnel diffraction formula⁵ from a set of holograms recorded by using a series of wavelengths. The numerical superposition of all the image volumes result in a synthesized short coherence length and corresponding axial resolution.^{6,7} The Fresnel diffraction formula, however, requires that the distance between the object and the hologram be sufficiently large in comparison to the size of the object or the hologram. This is referred to as the Fresnel approximation condition. Although the Fresnel diffraction formula can still give an accurate reconstruction for smooth and slowly varying objects where the Fresnel approximation is not strictly satisfied, it cannot correctly reconstruct near wave fields for more-diffractive objects, where the higher-order terms in the expansion of the Fresnel approximation are more significant. This places a stringent limit on the scanning range and specimen size and will adversely affect the signal-to-noise ratio of the tomographic sys-

tem as well. In this Letter, we describe a novel technique for overcoming these problems by incorporating the use of an angular spectrum method⁸⁻¹⁰ in our WSDIH system.

We start by briefly reviewing the principle of WSDIH. Suppose an object is illuminated by a laser beam of wavelength λ . A point P (at \mathbf{r}_P) on the object scatters the illumination beam into a Huygens wavelet $A(\mathbf{r}_P)\exp(ik|\mathbf{r}-\mathbf{r}_P|)$, where $A(\mathbf{r}_P)$ is proportional to the amplitude and phase of the scattered wavelet. For an extended object, the field at \mathbf{r} is

$$E(\mathbf{r}) \sim \int A(\mathbf{r}_P)\exp(ik|\mathbf{r}-\mathbf{r}_P|)d^3\mathbf{r}_P, \quad (1)$$

where the integral is over the object volume. The amplitude and phase of this field at the hologram plane $z=0$ is recorded by the hologram. If the holographic process is repeated using N different wavelengths and the reconstructed fields are all superposed together, then the resultant field is

$$E(\mathbf{r}) \sim \sum_k \int A(\mathbf{r}_P)\exp(ik|\mathbf{r}-\mathbf{r}_P|)d^3\mathbf{r}_P \\ \sim \int A(\mathbf{r}_P)\delta(\mathbf{r}-\mathbf{r}_P)d^3\mathbf{r}_P \sim A(\mathbf{r}). \quad (2)$$

That is, for a large enough number of wavelengths, the resultant field is proportional to the field at the object and is nonzero only at the object points. In practice, if one uses a finite number N of wavelengths at regular intervals of $\Delta(1/\lambda)$, then the object image $A(\mathbf{r})$ repeats itself (other than the diffraction-defocusing effect of propagation) at a beat wavelength $\Lambda=[\Delta(1/\lambda)]^{-1}$, with axial resolution $\delta=\Lambda/N$. By use of appropriate values of $\Delta(1/\lambda)$ and N , the beat wavelength Λ can be matched to the axial extent of the object and δ to the desired level of axial resolution.

The design of a WSDIH system is illustrated in Fig. 1, where a modified Mach-Zehnder interferometer apparatus is illuminated by a tunable dye laser.

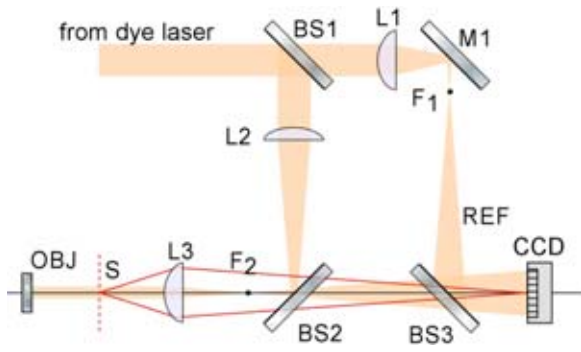


Fig. 1. Apparatus for the digital interference holography system: M1, mirror; OBJ, object; REF, reference.

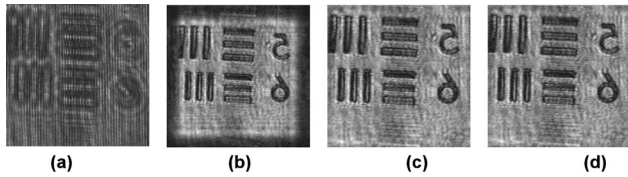


Fig. 2. (a) Hologram of a resolution target. Reconstructions from (b) the Fresnel diffraction formula, (c) Fresnel convolution, and (d) the angular spectrum method.

The input laser beam is split at beam splitter BS1 into reference and object beams, and each part is focused by lens L1 or L2 onto focal point F1 or F2. Point F2 is also the front focus of objective L3, so the object is illuminated with a collimated beam. The light scattered from the object travels through BS2 and BS3 and reaches the CCD camera. The reference beam's focus F1 is the same distance from BS3 as F2 is, so it is optically equivalent to a collimated beam incident from the left of objective L3. Plane S is imaged by L3 onto the camera, which records a magnified image of the interference pattern of the light scattered from the object onto S, through a distance z , and a plane-wave reference wave that would be present at S. The object and the reference beams are tilted with respect to each other in an off-axis hologram arrangement.

In our previous system,^{6,7} the Fresnel diffraction formula was used to calculate the wave field along the propagation direction. The resolution of the reconstructed images determined directly from the Fresnel diffraction formula will vary as a function of the reconstruction distance z as $\Delta x_o = \lambda z / (M \Delta x)$, where Δx and Δx_o are the resolutions of the hologram and the reconstructed image, respectively, and $M \times M$ is the array size of a square area on the CCD. To get consistent resolution, the Fresnel diffraction can also be implemented as a convolution. However, both of the above approaches assume the Fresnel approximation, which limits the flexibility and the signal-to-noise ratio of the system, as already mentioned. By using the angular spectrum algorithm for the WSDIH system, however, the problems associated with the Fresnel diffraction formula are solved.

From Fourier optics,¹⁰ if $E(x,y;0)$ is the object wave field at plane $z=0$, the corresponding angular spectrum of the object wave at this plane can be ob-

tained by taking the Fourier transform:

$$S(k_x, k_y; 0) = \iint E(x, y; 0) \exp[-i(k_x x + k_y y)] dx dy, \quad (3)$$

where k_x and k_y are the corresponding spatial frequencies of x and y . The object angular spectrum $S(k_x, k_y; 0)$ can be separated from other spectral components of the hologram with a bandpass filter if the off-axis angle θ of the incident beam is properly adjusted. The field $E(x, y; 0)$ can be rewritten as the inverse Fourier transform of its angular spectrum,

$$E(x, y; 0) = \iint S(k_x, k_y; 0) \exp[i(k_x x + k_y y)] dk_x dk_y. \quad (4)$$

The complex-exponential function $\exp[i(k_x x + k_y y)]$ may be regarded as a projection onto the plane $z=0$ of a plane wave propagating with a wave vector (k_x, k_y, k_z) , where $k_z = (k^2 - k_x^2 - k_y^2)^{1/2}$ and $k = 2\pi/\lambda$. Thus the field $E(x, y; 0)$ can be viewed as a projection of many plane-wave components propagating in different directions in space and with the complex amplitude of each component equal to $S(k_x, k_y; 0)$. After propagating along the z axis to a new plane, the new angular spectrum, $S(k_x, k_y; z)$, at plane z can be calculated as $S(k_x, k_y; 0) \exp(ik_z z)$. Thus the complex field distribution of any plane perpendicular to the propagating z axis can be calculated from Fourier theory as

$$E(x, y; z) = \iint S(k_x, k_y; z) \exp[i(k_x x + k_y y)] dk_x dk_y. \quad (5)$$

The resolution of the reconstructed images from the angular spectrum method is the same as that in the hologram plane. In spite of the apparent differences, the angular spectrum method will yield identical predictions of the diffracted field as the first Rayleigh–Sommerfeld solution.¹⁰ However, as an approximate Rayleigh–Sommerfeld solution, Fresnel diffraction is not capable of reconstructing the wave field near the hologram plane.

Figure 2(a) shows the hologram of a USAF-1951 resolution target with an area of $1.535 \text{ mm} \times 1.535 \text{ mm}$ and 256×256 pixels. The distance z representing the distance from the object to the hologram plane (S plane in Fig. 1) is 18 mm. The wave-

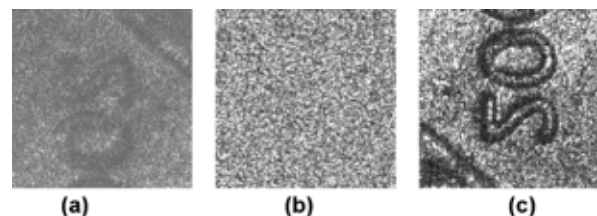


Fig. 3. (a) Hologram of a penny. Reconstructions from (b) Fresnel convolution and (c) the angular spectrum method.

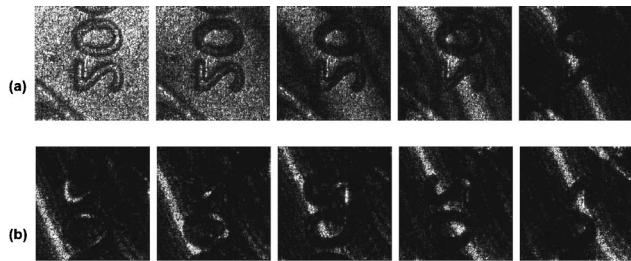


Fig. 4. (a) Buildup of axial resolution by superposition of holographic images with 1, 2, 4, 8, and 20 wavelengths. (b) Several contour images of the coin at $60 \mu\text{m}$ axial distance intervals.

length of the dye laser is 594 nm . The reconstructed resolution determined directly from the Fresnel diffraction formula is given by $\Delta x_o = \lambda z / M \Delta x \approx 7 \mu\text{m}$, which is slightly larger than the resolution of the hologram at $\Delta x = 6 \mu\text{m}$. Thus the reconstructed image (only amplitude is shown) is seen to be smaller in Fig. 2(b). However, reconstruction from either the Fresnel convolution or angular spectrum method has the same resolution as the hologram plane, as shown in Figs. 2(c) and 2(d). It is interesting to mention that, although the Fresnel approximation condition is not strictly satisfied in this example, the Fresnel diffraction can still give a fairly accurate reconstruction. This is because the resolution target is a relatively smooth and slowly varying object, with the major contribution to the wave field at the reconstructed point (x_o, y_o) coming from points (x, y) for which $x \approx x_o$ and $y \approx y_o$ on the hologram. The higher-order terms in the expansion of the Fresnel approximation, however, will be extremely important for a more diffractive object, which is most often the case for a WSDIH system in biological tomographic applications. In the following, we demonstrate the use of our WSDIH system in scanning a diffuse penny with an area of $2.62 \text{ mm} \times 2.62 \text{ mm}$. The reconstruction distance z is now 3.9 mm . To achieve the tomographic images, the wavelength of the dye laser is scanned within the range of $575.0\text{--}605.0 \text{ nm}$ in 20 steps. It gives an axial range of $\Lambda = 220 \mu\text{m}$ and a theoretical axial resolution of $\delta = 12 \mu\text{m}$, which fits well with its experimental value of $\sim 13 \mu\text{m}$ by reconstructing the wave distribution of a mirror along different axial distances and measuring the FWHM of the amplitude profile. Figure 3(a) shows the first hologram recorded with $\lambda = 575.0 \text{ nm}$, and Figs. 3(b) and 3(c) show the reconstructed amplitude from both the Fresnel convolution and the angular spectrum method, respectively. The results clearly show the significant advantage of the angular spectrum method in calculating wave fields near the hologram plane. In WSDIH, the optical field of a volume around the image location is calculated by the angular spectrum method for each wavelength. The 20 three-dimensional arrays are numerically superposed together, resulting in the accumulated field distribution that represents the three-dimensional

object structure. Figure 4(a) illustrates the buildup of axial resolution as a series of holographic images are superposed by using a range of wavelengths. One notices here the narrowing of the contour widths as the synthesized coherence length shortens. Figure 4(b) shows a few contour images at different axial distances.

In conclusion, we have shown that wave fields near the hologram plane can be accurately reconstructed for diffractive objects by using the angular spectrum method. Consequently, the tomographic system achieves a more flexible scanning range and more manageable specimen size selection. The sensitivity of our detection system is approximately 60 dB without image accumulation or lock-in, which is now lower than the performance of the standard OCT, ($\sim 100 \text{ dB}$) or full-field OCT ($\sim 90 \text{ dB}$),² where 200 images are locked in to obtain one tomographic image. As in the case of full-field OCT, the sensitivity of the WSDIH system is mainly limited by the electronic noise of the camera and the dynamic range of the CCD sensor, which is normally worse than those of photomultiplier tubes or photodiodes. The sensitivity can be greatly improved by using a CCD camera with higher dynamic range or incorporating binning or image lock-in techniques. The experiments presented above demonstrate that such three-dimensional tomographic images are obtained without the need for pixel-by-pixel scanning of the object volume. At this stage of development, the acquisition time is limited by the need to manually scan the laser wavelength. In the near future it can be accomplished by a motorized micrometer under computer control. Then the limiting factor of scanning will be the camera frame rate. In the above example, the calculation time used to obtain one tomographic image is $\sim 0.25 \text{ s}$, which can be greatly improved by using a parallel hardware system in the future.

The authors acknowledge financial support for this work from the National Science Foundation (DBI-0243237). The authors' e-mail addresses are yulingfeng@gmail.com and mkkim@cas.usf.edu.

References

1. D. Huang, E. A. Swanson, C. P. Lin, J. S. Schuman, W. G. Stinson, W. Chang, M. R. Hee, T. Flotte, K. Gregory, C. A. Puliafito, and J. G. Fujimoto, *Science* **254**, 1178 (1991).
2. A. Dubois, K. Grieve, G. Moneron, R. Lecaque, L. Vabre, and C. Boccara, *Appl. Opt.* **43**, 2874 (2004).
3. M. Ducros, M. Laubscher, B. Karamata, S. Bourquin, T. Lasser, and R. P. Salathe, *Opt. Commun.* **202**, 29 (2002).
4. L. Yu and M. K. Kim, *Opt. Express* **12**, 6632 (2004).
5. O. Schnars and W. Juptner, *Appl. Opt.* **33**, 179 (1994).
6. M. K. Kim, *Opt. Lett.* **24**, 1693 (1999).
7. M. K. Kim, *Opt. Express* **7**, 305 (2000).
8. L. Yu and L. Cai, *J. Opt. Soc. Am. A* **18**, 1033 (2001).
9. K. Matsushima, H. Schimmel, and F. Wyrowski, *J. Opt. Soc. Am. A* **20**, 1755 (2003).
10. J. W. Goodman, *Introduction to Fourier Optics* (McGraw-Hill, 1996).